


Structure of the HECT:ubiquitin complex and its role in ubiquitin chain elongation

Elena Maspero¹, Sara Mari¹, Eleonora Valentini¹, Andrea Musacchio², Alexander Fish³, Sebastiano Pasqualato^{2,4+} & Simona Polo^{1,5++}

¹IFOM, Fondazione Istituto FIRC di Oncologia Molecolare, ²Dipartimento di Oncologia Sperimentale, Istituto Europeo di Oncologia, Milan, Italy, ³Division of Biochemistry, The Netherlands Cancer Institute, Amsterdam, The Netherlands,

⁴Crystallography Unit, IFOM-IEO Campus, Cogentech—Consortium for Genomic Technologies, and ⁵Dipartimento di Medicina, Chirurgia ed Odontoiatria, Università degli Studi di Milano, Milan, Italy

 This is an open-access article distributed under the terms of the Creative Commons Attribution Noncommercial No Derivative Works 3.0 Unported License, which permits distribution and reproduction in any medium, provided the original author and source are credited. This license does not permit commercial exploitation or the creation of derivative works without specific permission.

Several mechanisms have been proposed for the synthesis of substrate-linked ubiquitin chains. HECT ligases directly catalyse protein ubiquitination and have been found to non-covalently interact with ubiquitin. We report crystal structures of the Nedd4 HECT domain, alone and in complex with ubiquitin, which show a new binding mode involving two surfaces on ubiquitin and both subdomains of the HECT N-lobe. The structures suggest a model for HECT-to-substrate ubiquitin transfer, in which the growing chain on the substrate is kept close to the catalytic cysteine to promote processivity. Mutational analysis highlights differences between the processes of substrate polyubiquitination and self-ubiquitination.

Keywords: catalysis; E3 ligase; polyubiquitination; structure; ubiquitin

EMBO reports (2011) 12, 342–349. doi:10.1038/embor.2011.21

INTRODUCTION

The ubiquitination process is carried out by an enzymatic cascade that includes an activating enzyme (E1), a conjugating enzyme (E2) and a ligase (E3; Dye & Schulman, 2007). The transfer of the

ubiquitin moiety from the thioester-linked E3 (in HECT-type ligases) to the acceptor lysine on the substrate is the last step of this process. Subsequent chain elongation requires the modification of specific lysine residues in consecutive ubiquitin moieties. With few exceptions (Petroski & Deshaies, 2005; Jin *et al*, 2008), little is known about the mechanisms of ubiquitin-chain assembly, although various models have been proposed (Hochstrasser, 2006).

The Nedd4 family of HECT domain E3 ligases is a well-characterized class of enzymes that present a conserved modular organization with an amino-terminal C2 domain that is crucial for membrane localization, between two and four WW domains that recognize substrates and adaptor proteins and a carboxy-terminal catalytic HECT domain. In humans, there are nine members of this family that are implicated in a range of biological processes such as endocytosis, protein transport, viral budding, signalling, cellular growth and proliferation (Rotin & Kumar, 2009). This class of E3 enzymes seems to use a sequential addition mechanism, by which ubiquitin molecules are added one at a time from the catalytic cysteine to the distal lysine of the growing chain (Kim & Huibregtse, 2009). A key question is how E3 enzymes deal with the shifting position of the acceptor site during chain elongation.

Two groups have recently identified a surface implicated in non-covalent ubiquitin binding on the HECT-type E3 ligases Rsp5 and Smurf2 (French *et al*, 2009; Ogunjimi *et al*, 2010). This surface was proposed to have a role in regulating polyubiquitination, although opposite mechanisms were suggested by the groups, with the surface being required to either restrict the length of polyubiquitin chains synthesized by the HECT domain (French *et al*, 2009) or to promote polyubiquitination (Ogunjimi *et al*, 2010). In this study, we show the crystal structure of the HECT domain of Nedd4 alone and in complex with ubiquitin, and we present molecular insights into the mechanism by which Nedd4 catalyses polyubiquitination.

¹IFOM, Fondazione Istituto FIRC di Oncologia Molecolare,

²Dipartimento di Oncologia Sperimentale, Istituto Europeo di Oncologia, Via Adamello 16, Milan 20139, Italy

³Division of Biochemistry, The Netherlands Cancer Institute, Plesmanlaan 121, Amsterdam 1066 CX, The Netherlands

⁴Crystallography Unit, IFOM-IEO Campus, Cogentech—Consortium for Genomic Technologies, Via Adamello 16, Milan 20139, Italy

⁵Dipartimento di Medicina, Chirurgia ed Odontoiatria, Università degli Studi di Milano, Via di Rudini 8, Milan 20122, Italy

+Corresponding author. Tel: +39 02 94375172; Fax: +39 02 94375990;

E-mail: sebastiano.pasqualato@ifom-ieo-campus.it

++Corresponding author. Tel: +39 02 574303242; Fax: +39 02 574303231;

E-mail: simona.polo@ifom-ieo-campus.it

Received 23 July 2010; revised 4 January 2011; accepted 13 January 2011; published online 11 March 2011

RESULTS AND DISCUSSION

Structure of HECT^{Nedd4} and HECT^{Nedd4}:ubiquitin

We characterized the interaction of the isolated HECT domain of Nedd4 (HECT^{Nedd4}) with ubiquitin in detail. The ubiquitin-binding ability resides in the N-lobe, does not show preference for Lys 63- or Lys 48-polyubiquitin chains and requires the canonical hydrophobic patch on ubiquitin, centred on Ile 44 (supplementary Fig S1 online). We extended this analysis to the other mammalian Nedd4 family members and found that only a subset of these HECT domains binds to ubiquitin, namely Nedd4, Nedd4-like and Smurf2 (Fig 1A).

To understand how ubiquitin binds to the HECT, we determined the crystal structure of the HECT^{Nedd4} in isolation (at 2.5 Å) and in complex with ubiquitin (at 2.7 Å) by molecular replacement (supplementary Table S1 online and supplementary Fig S2 online). In both structures, HECT^{Nedd4} displays the typical HECT fold (Huang *et al*, 1999; Verdecia *et al*, 2003; Ogunjimi *et al*, 2005) composed of two lobes connected by a flexible hinge (Fig 1B,C). The N-lobe, an elongated array of helices and β -hairpins, consists of two moieties, known as the large and small subdomains (Fig 1B). The small subdomain, which hosts the E2-binding site, comprises helices $\alpha 6$ – $\alpha 8$ and β -sheets $\beta 5$ – $\beta 6$ (Huang *et al*, 1999; Kamadurai *et al*, 2009). The large subdomain of the N-lobe is present below the C-lobe, an α/β sandwich domain that carries the catalytic cysteine. The orientation of the C-lobe differs in the two HECT^{Nedd4} structures, and both orientations are distinct from those of previously reported HECT domain structures (supplementary Fig S3 online). This highlights the freedom of movement of the C-lobe, which is key for the catalytic function of HECT domains (Verdecia *et al*, 2003; Kamadurai *et al*, 2009).

Non-covalent ubiquitin binding to HECT^{Nedd4} conceals a solvent-accessible interaction surface area on ubiquitin of approximately 900 Å², the largest surface identified so far for ubiquitin-binding domains (supplementary Table S2 online). Ubiquitin makes contact with Glu 554 and neighbouring residues of helix $\alpha 1$; Tyr 604, Tyr 605 and Tyr 610 from the region comprising helix $\alpha 3'$ and strand $\beta 3$; Asn 628 and Glu 629 from helix $\alpha 4'$ and the ensuing loop; and Phe 707 and neighbouring residues of the $\beta 5$ – $\beta 6$ beta hairpin. These residues are distributed in both the small and the large subdomains of the N-lobe (Figs 1E,2A). In the absence of ubiquitin, the relative orientation of the small and large subdomains is not fixed and varies for different structures (Huang *et al*, 1999; Verdecia *et al*, 2003; Ogunjimi *et al*, 2005). Ubiquitin binding might therefore be expected to stabilize a specific reciprocal orientation of the N-lobe subdomains. Indeed, superposition of the large subdomains of HECT^{Nedd4} and HECT^{Nedd4}:ubiquitin (root mean square deviation of 0.6 Å over 181 C α) clearly indicates a relative movement of the $\beta 5$ – $\beta 6$ hairpin of the small subdomain in the HECT^{Nedd4}:ubiquitin structure by approximately 5 Å towards the large subdomain of the N-lobe (Fig 1D).

As predicted by the defective behaviour of the I44A ubiquitin mutant (supplementary Fig S1C online), the interaction surface on ubiquitin involves the canonical Ile 44 hydrophobic patch, which also includes Gly 47, Leu 8 and Val 70 (Fig 2A). However, the surface of interaction is not limited to this patch, but extends to a 'second hydrophobic patch', including the residues Ile 36/Leu 71/Leu 73, the role of which has recently been discussed in the context of the E2-to-HECT ubiquitin transfer (Kamadurai *et al*,

2009; Fig 2A; supplementary Fig S4 online). The Asn 628, Tyr 634 and Glu 554 side chains on Nedd4 form hydrogen bonds with the main chain nitrogen atoms of ubiquitin-Leu 73, Arg 74 and Gly 75, whereas the ubiquitin-Leu 73 side chain is stacked between Tyr 634 and Tyr 605 of Nedd4.

We generated Nedd4 mutants that substantiate the functional importance of both interacting patches on ubiquitin. Mutation of Tyr 605 to Ala (Y605A) or Phe 707 to Ala (F707A) almost abolished HECT^{Nedd4} binding to Lys 63 ubiquitin (Fig 2B). Phe 707 to Tyr (F707Y), Asn 628 to Ala (N628A) or Glu 629 to Ala (E629A) mutations had milder effects, preserving the association with higher molecular weight Lys 63 ubiquitin to varying degrees (Fig 2B). We confirmed these results by measuring the interaction between the HECT domains and monomeric and dimeric ubiquitin by fluorescence polarization and surface plasmon resonance (SPR) assay (Fig 2C; supplementary Fig S1D–F online). Both ubiquitin ligands interact with the HECT with rapid kinetics (fast K_{on} and K_{off} rate constants, data not shown). Wild-type HECT^{Nedd4} displays a moderate affinity (K_D approximately 11 μ M) in the range of those reported for ubiquitin-binding domains (supplementary Table S2 online), whereas Y605A and F707A mutations show from 20- to 30-fold decreases in binding (Fig 2C; supplementary Fig S1F online).

Role of ubiquitin binding in Nedd4 activity

Next, we analysed the catalytic activity of Nedd4 HECT mutants. In principle, the ubiquitin-binding surface might have a role at three stages of the E3 catalysis: binding to the E2, transthiolation process from E2 to E3 or substrate ubiquitination. We tested all of these possibilities using the isolated HECT, which retains the ability to ubiquitinate itself as well as substrates, albeit with reduced efficiency (not shown).

Pull-down and SPR assays showed that mutants have no significant impairment in binding with either the apo or the ubiquitin thioester-linked form of E2 enzyme Ube2D3 (Fig 3A and data not shown). Indeed, the E2 binding is built on an adjacent but non-overlapping surface on the large subdomain of the N-lobe (Huang *et al*, 1999; Fig 4C). We then tested the importance of the ubiquitin-binding surface in the E2-to-HECT transthiolation process by using a pulse-chase protocol (Fig 3B). Again, no appreciable transthiolation defects were observed for the mutants, supporting the notion that the ubiquitin-binding surface is not involved in the upstream steps of the enzymatic cascade. Of note, the thioester HECT~ubiquitin bond is unstable and the ubiquitin moiety is immediately transferred to the lysine/s of the HECT, as demonstrated by the appearance of higher molecular-weight proteins that are resistant to dithiothreitol treatment (Fig 3B, lower panels).

These results led us to propose that the ubiquitin-binding surface on the HECT might act to bind a ubiquitin moiety that is already conjugated to a substrate, thus promoting polyubiquitination. Indeed, when we assayed F707A and Y605A in an *in vitro* ubiquitination reaction, we found that mutations in the ubiquitin-binding surface strongly impaired free-chain formation and ubiquitination of all the substrates tested (Fig 3C; supplementary Fig S5 online). The mutant enzymes were efficient in the first cycle of substrate ubiquitination and in ubiquitin dimer formation, using free ubiquitin as a pseudosubstrate (Fig 3C; supplementary Fig S5 online). This was confirmed by using a ubiquitin Lys 0 mutant and

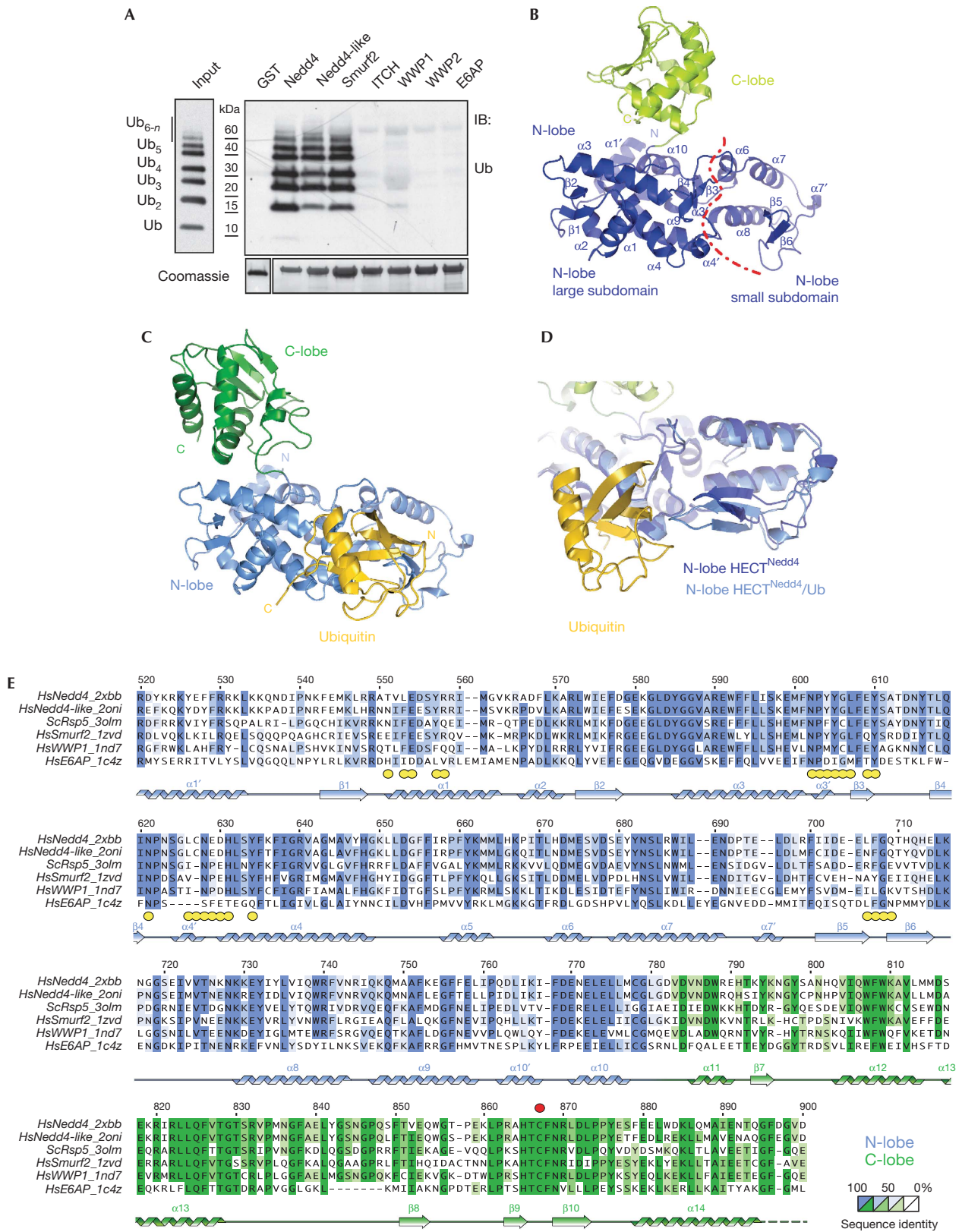


Fig 1 | Structure of the HECT^{Nedd4} domain in apo form and in complex with ubiquitin. (A) GST pull-down assay with the HECT domains of various Nedd4 family HECT E3 ligases. GST-fusion proteins were incubated for 2 h at 4 °C in YY buffer with synthetic Lys 63-polyubiquitin chains and analysed by IB as indicated. Coomassie staining shows comparable loading of GST proteins. Similar results were obtained with linear and Lys 48-polyubiquitin chains (not shown). (B) Overall structure of HECT^{Nedd4} (N-lobe, blue; C-lobe, green). The red dotted line indicates the boundary between the large and small subdomains of the N-lobe. (C) Overall structure of HECT^{Nedd4} in complex with ubiquitin (yellow). The HECT structure is represented in the same orientation as in B; N-lobe, light blue; C-lobe, dark green. (D) Superposition on the large subdomain of the N-lobe of HECT^{Nedd4} and HECT^{Nedd4}:ubiquitin. In the complex (light blue), the β 5- β 6 hairpin of the small subdomain of the N-lobe is closer to the large subdomain, with respect to the isolated HECT (dark blue). (E) Sequence alignment of the HECT^{Nedd4} domain with other crystallized HECT domains. Secondary structure elements are depicted. Dotted line indicates that the residues were not visible in the electron density maps. Yellow circles indicate residues in contact with ubiquitin in the structure of HECT^{Nedd4}:ubiquitin (according to PISA; Krissinel & Henrick, 2007). Numbering refers to Nedd4 sequence. GST, glutathione S-transferase; IB, immunoblotting; Ub, ubiquitin.

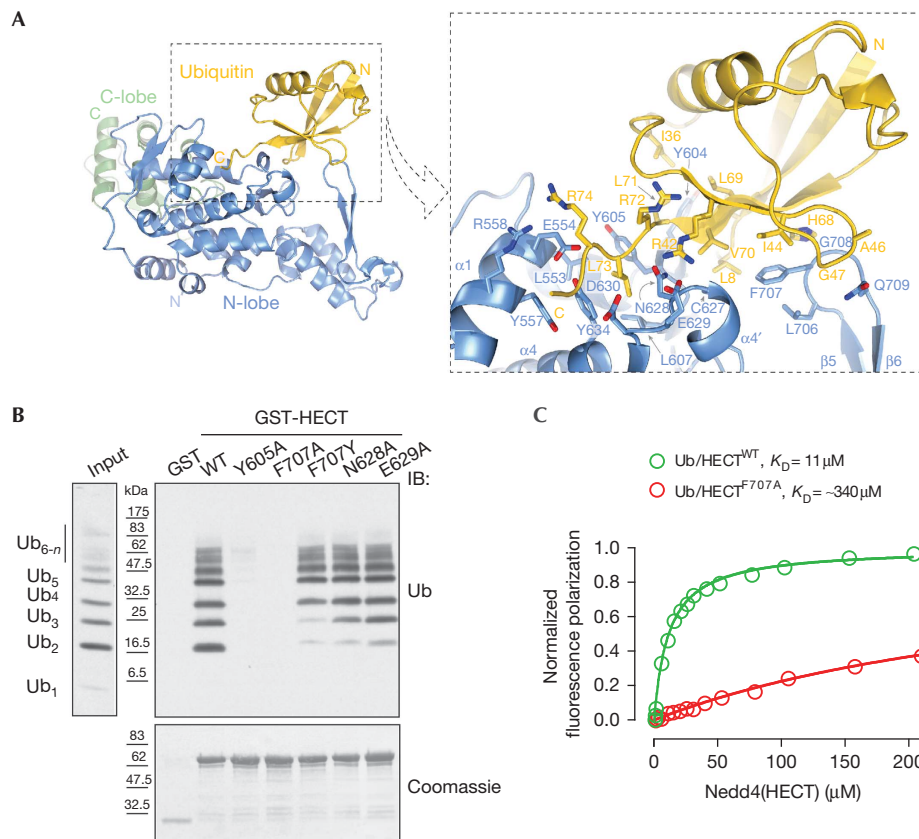


Fig 2 | HECT^{Nedd4}:ubiquitin interaction and mutant validation. (A) Close-up view of HECT^{Nedd4} N-lobe:ubiquitin interaction. (B) GST pull-down assay with the indicated Nedd4 constructs and Lys 63-linked polyubiquitin chains was performed as described in Fig 1A. (C) Fluorescence-polarization assay with the indicated Nedd4 constructs and monomeric ubiquitin was performed. The HECT^{Nedd4}:ubiquitin interaction displays a moderate affinity with a K_D of 11 μM , F707A mutant displays a thirty times lower affinity. Details are described in the supplementary Methods online and similar results for the Y605A mutant obtained by SPR assay are in supplementary Fig S1 online. IB, immunoblotting; GST, glutathione S-transferase; SPR, surface plasmon resonance; Ub, ubiquitin; WT, wild type.

quantification of the results repeated as fold differences between wild-type HECT and mutants (supplementary Fig S5A online). Interestingly, F707A and Y605A mutations did not affect self-ubiquitination of Nedd4 (Fig 3B, lower panels and Fig 3D), indicating that this *in cis* reaction is a catalytically distinct process that cannot be used as a surrogate assay for ligase activity on substrates.

Most HECT E3s synthesize polyubiquitin chains with specific linkages (Wang *et al*, 2006; Kim *et al*, 2007). To gain insight into

the type of chains synthesized by Nedd4, we tested substrate ubiquitination using ubiquitin-bearing individual lysine-to-arginine mutations (KR mutants). We found that Nedd4 has a strong preference for building Lys 63-chains on substrates, a feature retained by the F707A mutant (Fig 4A). Consistent with previous data, however, F707A has defective chain elongation on substrate and shorter free chains, regardless of the type of ubiquitin used (Fig 4A). Therefore, we conclude that the ubiquitin-binding surface on the HECT acts to promote substrate polyubiquitination,

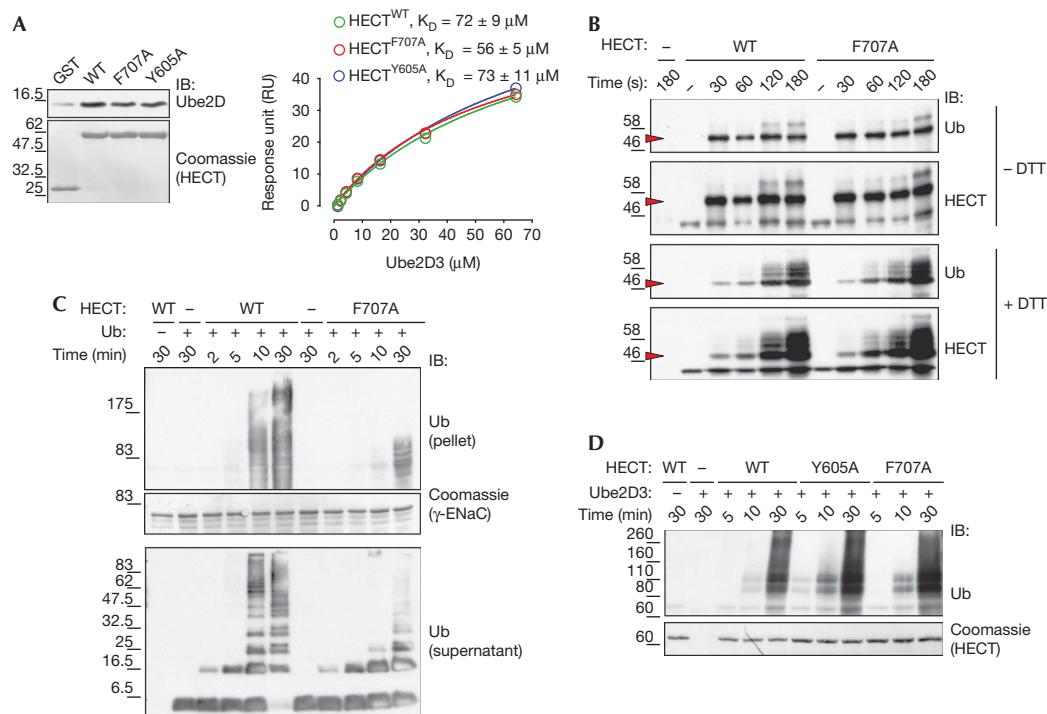


Fig 3 | Disruption of HECT^{Nedd4}:ubiquitin interaction impairs substrate polyubiquitination. (A) Mutations do not affect E2 binding. Left panel: GST pull-down assay with the indicated HECT mutants and the E2 enzyme Ube2D3. IB was performed as indicated. Coomassie staining shows comparable loading of GST proteins. Right panel: the HECT^{Nedd4}:Ube2D3 interaction displays a modest affinity, that is not perturbed by the F707A and Y605A mutations. SPR assay was performed as described in the supplementary methods online. (B) Mutations do not affect the kinetics of the E2-to-HECT transthioylation process. The transfer of ubiquitin was monitored by quenching the reaction at different time points, with the addition of Laemmli buffer with or without the reducing agent (100 mM DTT). Arrow indicates thioester HECT~ubiquitin (–DTT) or monoubiquitinated HECT (+DTT) running at the same position. DTT-resistant higher molecular bands represent self-ubiquitinated HECT. Similar results were obtained with Y605A mutant. (C) Mutations impair substrate polyubiquitination. Upper panel: GST- γ ENaC ubiquitination kinetics with WT HECT and F707A mutant (ubiquitin (pellet)). Middle panel: Coomassie staining showing comparable loading of GST proteins. Lower panel: kinetics of free ubiquitin chain formation (ubiquitin (supernatant)) during the reaction. IB was performed as indicated. (D) Self-ubiquitination kinetics with WT HECT and Y605A and F707A mutants. IB was performed as indicated. Coomassie staining shows comparable loading of HECT proteins. Similar results were obtained with full-length Nedd4 mutants. DTT, dithiothreitol; ENaC, epithelial Na⁺ channel; GST, glutathione S-transferase; IB, immunoblotting; SPR, surface plasmon resonance; Ub, ubiquitin; WT, wild type.

but it does not dictate the preference for a specific lysine during elongation. Indeed, recent observations suggest that the C-lobe, rather than the ubiquitin-binding N-lobe, is the crucial determinant of lysine selection during elongation (Kim & Huibregtse, 2009).

CONCLUSIONS

Collectively, our results support the hypothesis that the ubiquitin-binding surface is required for the processivity of the polyubiquitination reaction (Ogunjimi *et al*, 2010), rather than for limiting chain elongation, as suggested previously (French *et al*, 2009). How can this occur? It is tempting to envision a model in which the distal ubiquitin on the substrate occupies this surface, promoting retention of the ubiquitinated substrate to the E3, and also keeping the small subdomain of the N-lobe in a conformation that favours processive ubiquitin addition. This could be achieved by either reducing the gap between the catalytic cysteine of the HECT and the C-terminus of ubiquitin linked to the E2 enzyme (Kamadurai *et al*, 2009) or by facilitating the transfer of a

subsequent ubiquitin to the HECT-bound substrate. In support of this model, we found that the non-covalent ubiquitin-binding surface that we mapped remains accessible in the complex of the HECT domain of Nedd4-like with the ubiquitin-loaded E2 (Kamadurai *et al*, 2009; Fig 4C).

Our data support the notion that Nedd4 adopts a simple sequential-addition model to build a chain on a substrate; after the first ubiquitin is attached, the chain is elongated through Lys 63 linkage, because of the ability of the N-lobe to maintain the growing polyubiquitin chain in close proximity. A similar conclusion about the role of the HECT ubiquitin-binding site in promoting chain elongation was reached in the accompanying study by Kim *et al* (2011) on Rsp5. Although the position of Lys 63 on bound ubiquitin does not seem to be able to orient the growing chain towards the E2 catalytic cysteine (Fig 4B), the average B factors for the ubiquitin molecules are considerably higher than those of their HECT counterparts (approximately 76 Å² for ubiquitin molecules, approximately 48 Å² for HECT domains; supplementary Table S1 online), suggesting freedom of movement of ubiquitin on its docking site. This could imply that the binding of

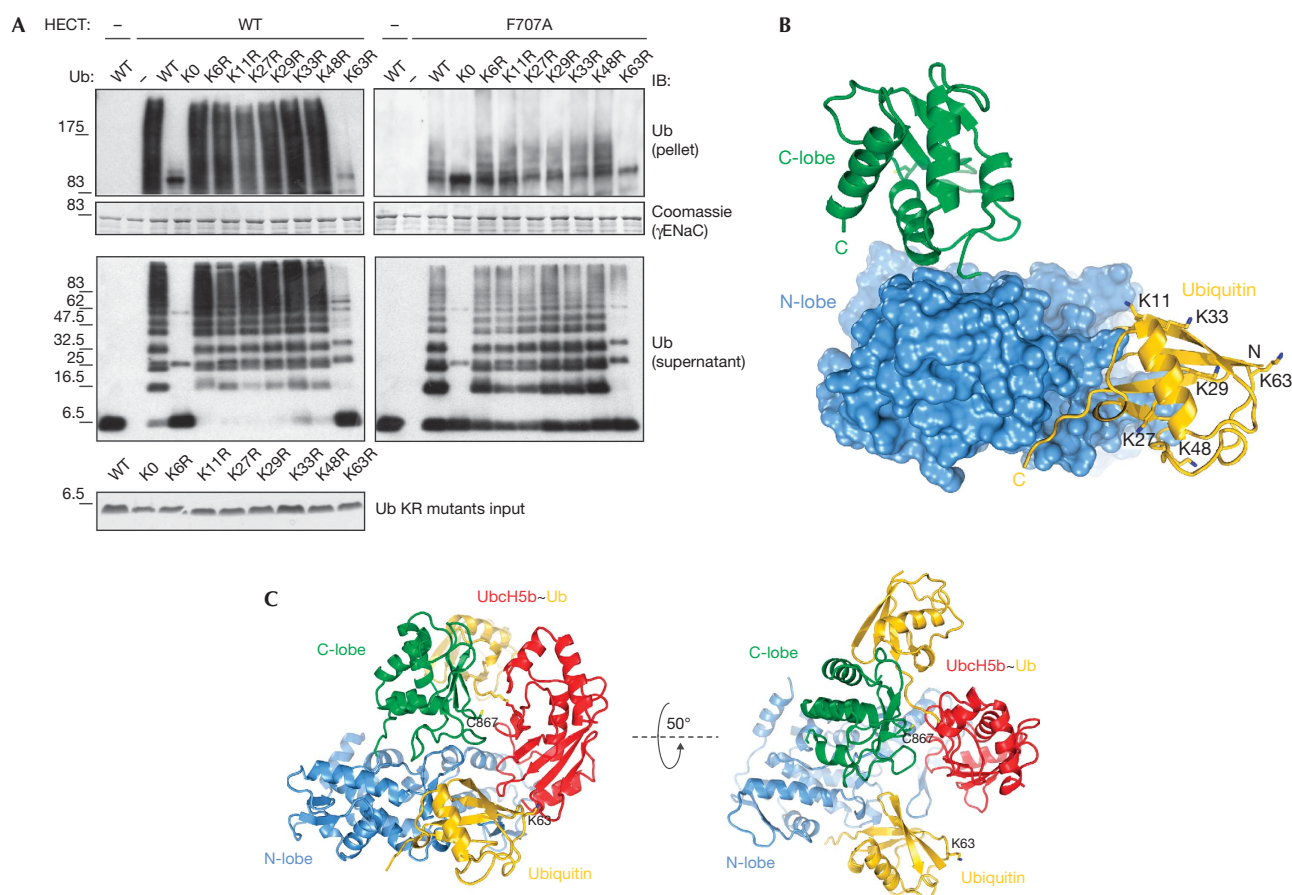


Fig 4 | Ubiquitin binding to the HECT^{Nedd4} domain is compatible with HECT^{Nedd4}-like:E2~ubiquitin complex and does not dictate chain specificity. (A) Substrate ubiquitination assay with the indicated ubiquitin KR mutants was performed. The reaction was quenched after 30 min for the WT HECT and after 60 min for the F707A mutant. Upper panel: GST- γ ENaC ubiquitination with the indicated constructs. Middle panel: Coomassie staining showing comparable loading of GST proteins. Lower panel: free ubiquitin chain formation during the reaction. IB was performed as indicated. Lower panel: 1 μ g of ubiquitin KR mutants were loaded for comparison and visualized by Coomassie staining. (B) Position of ubiquitin lysines in the Nedd4 HECT/ubiquitin complex. HECT N-lobe is shown as surface representation, whereas the C-lobe and ubiquitin are shown as cartoon representations. Ubiquitin lysine side chains are indicated in sticks. Six of the seven ubiquitin lysines are shown, K6 being in the back. (C) Model of Ubch5b~Ub:C-lobe complex (Kamadorai et al, 2009) binding to the N-lobe:ubiquitin complex. Details are in the supplementary Methods online. C867 on the HECT and K63 on the Ub are shown. ENaC, epithelial Na⁺ channel; GST, glutathione S-transferase; IB, immunoblotting; KR, lysine-to-arginine mutation; Ub, ubiquitin; WT, wild type.

ubiquitin to the E3 is strong enough to promote polyubiquitination, yet loose enough to allow chain growth, possibly through a slippage mechanism by which the ubiquitin-binding surface specifically binds to the distal ubiquitin at the end of the chain. The moderate affinity and fast kinetic rates of the HECT:ubiquitin interaction fit well with such a mechanism. Future structural studies with Nedd4 in complex with a ubiquitinated substrate might be required to provide a definitive picture of this dynamic process.

The detailed molecular view provided by our structure allows the identification of the crucial residues required for binding (Fig 1E), which can be used to predict the HECT E3 enzymes that are able to bind to ubiquitin. It remains to be established whether the presence of this binding surface might determine the mechanism of chain synthesis adopted by the different HECT ligases to become processive.

At our level of understanding, generalizing the mechanisms that underlie polyubiquitination would be premature, but it is

interesting to note from the comparison of the small Nedd4 family of E3, that nature has used a variety of protein architectures to ensure specificity.

METHODS

Crystallization and structure determination. Crystals of HECT^{Nedd4} and HECT^{Nedd4}:ubiquitin complex were obtained by sitting-drop vapour diffusion at 20 °C, using a Honeybee Cartesian robot in 96-well plates. Diffraction-quality crystals were obtained by optimizing the initial conditions in 24-well plates, hanging drops at 20 °C. Crystals were all optimized by microseeding. For HECT^{Nedd4}, the optimized conditions were 100 mM Na-MES, pH 6.0, 2–4% PEG 400 or PEG 600, 30–60 mM CaCl₂ or MgCl₂, 5 mM tris(2-carboxyethyl)phosphine, with protein concentration in the 2.5–5 mg/ml range. Crystals were cryoprotected in 100 mM Na-MES, pH 6.0, 4% PEG 400, supplemented with 20% ethylene glycol. The structure was solved with a data set collected at the European

Synchrotron Radiation Facility (ESRF) at beamline ID14-2. For the HECT^{Nedd4}:ubiquitin complex, initial crystals were obtained in 100 mM Na-HEPES, pH 7–8, 10–20% PEG 2000 MME, 5 mM tris(2-carboxyethyl)phosphine, with proteins purified individually, then mixed in a 1:1 molar ratio and a concentration of approximately 30 mg/ml. To obtain good-quality diffraction and to overcome twinning, the complex was crystallized in the presence of excess ubiquitin (600–900 μ M of complex, $1.2 \times -2.3 \times$ ubiquitin molar excess), lower concentration of PEG 2000 MME (2–10%), and the crystals were carefully frozen by equilibrating them into cryo-buffer (100 mM Na-HEPES, pH 7.5, 10% PEG 2000 MME) with increasing concentrations of glycerol, reaching a final concentration of 20%. The structure was solved with a data set collected at the ESRF at beamline ID14-1 on a crystal grown in a $1.9 \times$ ubiquitin molar excess.

X-ray diffraction data were processed with HKL2000 (Otwinowski & Minor, 1997) or XDS (Kabsch, 2010). Both structures were solved by molecular replacement with Phaser within the CCP4 suite (CCP4, 1994), using as a search model the HECT domain of Nedd4-like (Protein Data Bank entry 2oni) in the case of HECT^{Nedd4}, and HECT^{Nedd4} and a high-resolution structure of ubiquitin (Protein Data Bank entry 1ubi) in the case of HECT^{Nedd4}:ubiquitin complex. Initial models were refined with the CNS suite (Brunger, 2007), Refmac (Murshudov *et al*, 1997), the Phenix suite (Adams *et al*, 2010) and manual building in Coot (Emsley *et al*, 2010). For the HECT^{Nedd4}:ubiquitin complex, non-crystallographic symmetry (NCS) restraints were used in refinement. In the first cycles of refinement carried out with Refmac, HECT molecules were divided into two NCS groups (the N-lobe and the C-lobe), and ubiquitin molecules were the third NCS group. For further refinement cycles carried out with phenix.refine, five NCS groups were used: ubiquitin molecules and HECT domain residues 522:699, 724:778, 785:828 and 850:891, thus not subjecting HECT domain loops to NCS restraints. Structure representations were generated with Pymol (DeLano Scientific LLC). HECT^{Nedd4} crystallized in spacegroup C2, whereas HECT^{Nedd4}:ubiquitin crystallized in spacegroup P2₁, with two complexes per asymmetrical unit. The two complexes differ slightly in the orientation of the HECT^{Nedd4} C-lobe with respect to the N-lobe, and the relative orientation of HECT^{Nedd4} with respect to ubiquitin, but the interactions discussed here are present in both complexes. Superpositions of pairs of domains of the asymmetrical unit indicate that they are almost identical (root mean square deviations of N-lobes: 0.36 Å over 260 C _{α} ; C-lobes: 0.63 Å over 115 C _{α} ; Ubs: 0.25 Å over 76 C _{α}).

Ubiquitination assay. Ubiquitination assays were performed with HECT domains produced as glutathione S-transferase (GST) fusion proteins and cleaved with PreScission protease. The E2 enzyme Ube2D3, was produced as a His₆-fusion protein and eluted from Ni-NTA Agarose beads (Qiagen). Reaction mixtures contained purified enzymes (20 nM E1, 250 nM of purified His₆-tagged Ube2D3, 250 nM HECT^{Nedd4}), 300 nM of substrate (γ epithelial Na⁺ channel and LMP2A were produced as GST fusion proteins and used attached to glutathione beads) and 1 μ M of ubiquitin in ubiquitination buffer (25 mM Tris-HCl, pH 7.6, 5 mM MgCl₂, 100 mM NaCl, 0.2 μ M dithiothreitol, 2 mM ATP). Reactions were incubated at 37 °C. At the indicated time point, samples were centrifuged to separate the pellet—containing the ubiquitinated substrates—and the supernatant—containing the enzymes and the

soluble ubiquitin chains, if produced. The pellet was washed four times in YY buffer (50 mM Na-HEPES pH 7.5, 150 mM NaCl, 1 mM EDTA, 10% glycerol, 1% triton X-100) before loading on SDS-polyacrylamide gel electrophoresis gel. For self-ubiquitination reaction, the mixtures contained 20 nM E1, 250 nM of purified His₆-tagged Ube2D3, 250 nM of GST-HECT^{Nedd4} and 0.5 μ M of ubiquitin in ubiquitination buffer. Detection was performed by immunoblotting using specific antibody. Coomassie-stained membrane was used to show loading of GST-fusion protein after immunoblotting.

Reagents and constructs, protein expression and purification, transthiolation assay, pull-down experiments, fluorescence polarization assay and SPR are described in the supplementary Methods online.

Accession codes: Coordinates for HECT^{Nedd4} and the HECT^{Nedd4}:ubiquitin complex have been deposited at the Protein Data Bank under accession codes 2xbf and 2xbb, respectively.

Supplementary information is available at EMBO reports online (<http://www.emboreports.org>).

ACKNOWLEDGEMENTS

We thank P.R. Romano for critically reading the manuscript, V. Cecatiello for assistance in crystallization, R.A. Steiner for advice, the staff at European Synchrotron Radiation Facility for assistance in data collection and M.P.A. Luna-Vargas for providing reagents. This work was supported by grants from the Associazione Italiana per la Ricerca sul Cancro (AIRC) and the European Community (FP7) to S.P. E.M. is the recipient of an AIRC fellowship.

CONFLICT OF INTEREST

The authors declare that they have no conflict of interest.

REFERENCES

- Adams PD *et al* (2010) PHENIX: a comprehensive Python-based system for macromolecular structure solution. *Acta Crystallogr D Biol Crystallogr* **66**: 213–221
- Brunger AT (2007) Version 1.2 of the Crystallography and NMR system. *Nat Protoc* **2**: 2728–2733
- CCP4 (1994) The CCP4 suite: programs for protein crystallography. *Acta Crystallogr D Biol Crystallogr* **50**: 760–763
- Dye BT, Schulman BA (2007) Structural mechanisms underlying posttranslational modification by ubiquitin-like proteins. *Annu Rev Biophys Biomol Struct* **36**: 131–150
- Emsley P, Lohkamp B, Scott WG, Cowtan K (2010) Features and development of Coot. *Acta Crystallogr D Biol Crystallogr* **66**: 486–501
- French ME, Kretzmann BR, Hicke L (2009) Regulation of the RSP5 ubiquitin ligase by an intrinsic ubiquitin-binding site. *J Biol Chem* **284**: 12071–12079
- Hochstrasser M (2006) Lingering mysteries of ubiquitin-chain assembly. *Cell* **124**: 27–34
- Huang L, Kinnucan E, Wang G, Beaudenon S, Howley PM, Huibregtse JM, Pavletich NP (1999) Structure of an E6AP-UbcH7 complex: insights into ubiquitination by the E2-E3 enzyme cascade. *Science* **286**: 1321–1326
- Jin L, Williamson A, Banerjee S, Philipp I, Rape M (2008) Mechanism of ubiquitin-chain formation by the human anaphase-promoting complex. *Cell* **133**: 653–665
- Kabsch W (2010) Xds. *Acta Crystallogr D Biol Crystallogr* **66**: 125–132
- Kamadurai HB, Souphron J, Scott DC, Duda DM, Miller DJ, Stringer D, Piper RC, Schulman BA (2009) Insights into ubiquitin transfer cascades from a structure of a UbcH5B approximately ubiquitin-HECT(NEDD4L) complex. *Mol Cell* **36**: 1095–1102
- Kim HC, Huibregtse JM (2009) Polyubiquitination by HECT E3s and the determinants of chain type specificity. *Mol Cell Biol* **29**: 3307–3318

- Kim HT, Kim KP, Lledias F, Kisselev AF, Scaglione KM, Skowrya D, Gygi SP, Goldberg AL (2007) Certain pairs of ubiquitin-conjugating enzymes (E2s) and ubiquitin-protein ligases (E3s) synthesize nondegradable forked ubiquitin chains containing all possible isopeptide linkages. *J Biol Chem* **282**: 17375–17386
- Kim HY, Steffen AM, Oldham ML, Chen J, Huibregtse JM (2011) Structure and function of an HECT domain ubiquitin-binding site. *EMBO Rep* **12**: 334–341
- Krissinel E, Henrick K (2007) Inference of macromolecular assemblies from crystalline state. *J Mol Biol* **372**: 774–797
- Murshudov GN, Vagin AA, Dodson EJ (1997) Refinement of macromolecular structures by the maximum-likelihood method. *Acta Crystallogr D Biol Crystallogr* **53**: 240–255
- Ogunjimi AA, Briant DJ, Pece-Barbara N, Le Roy C, Di Guglielmo GM, Kavsak P, Rasmussen RK, Seet BT, Sicheri F, Wrana JL (2005) Regulation of Smurf2 ubiquitin ligase activity by anchoring the E2 to the HECT domain. *Mol Cell* **19**: 297–308
- Ogunjimi AA, Wiesner S, Briant DJ, Varelas X, Sicheri F, Forman-Kay J, Wrana JL (2010) The ubiquitin binding region of the Smurf HECT domain facilitates polyubiquitylation and binding of ubiquitylated substrates. *J Biol Chem* **285**: 6308–6315
- Otwinowski Z, Minor W (1997) Processing of X-ray diffraction data collected in oscillation mode. *Methods Enzymol* **276**: 307–326
- Petroski MD, Deshaies RJ (2005) Mechanism of lysine 48-linked ubiquitin-chain synthesis by the cullin-RING ubiquitin-ligase complex SCF–Cdc34. *Cell* **123**: 1107–1120
- Rotin D, Kumar S (2009) Physiological functions of the HECT family of ubiquitin ligases. *Nat Rev Mol Cell Biol* **10**: 398–409
- Verdecia MA, Joazeiro CA, Wells NJ, Ferrer JL, Bowman ME, Hunter T, Noel JP (2003) Conformational flexibility underlies ubiquitin ligation mediated by the WWP1 HECT domain E3 ligase. *Mol Cell* **11**: 249–259
- Wang M, Cheng D, Peng J, Pickart CM (2006) Molecular determinants of polyubiquitin linkage selection by an HECT ubiquitin ligase. *EMBO J* **25**: 1710–1719



EMBO reports is published by Nature Publishing Group on behalf of European Molecular Biology Organization.

This article is licensed under a Creative Commons Attribution Noncommercial No Derivative Works 3.0 Unported License [<http://creativecommons.org/licenses/by-nc-nd/3.0>]